



XVIIth World Congress of the International Commission of Agricultural and Biosystems Engineering (CIGR)

Hosted by the Canadian Society for Bioengineering (CSBE/SCGAB)
Québec City, Canada June 13-17, 2010



A DEVICE FOR EXTRACTING 3D INFORMATION OF FERTILIZER TRAJECTORIES

B. HIJAZI^{1,2}, J. BAERT², F. COINTAULT¹, J. DUBOIS³, M. PAINDAVOINE⁴,
J. PIETERS⁵, J. VANGEYTE²

¹AgroSup Dijon – UP GAP – 26, Bd Dr Petitjean – BP 87999 – 21079 Dijon cedex – France

²Institute for Agricultural and Fisheries Research (ILVO) - Technology and Food Science Unit – Agricultural Engineering – Burg. Van Gansberghelaan 115 – 9820 Merelbeke – Belgium

³Le2i – UMR CNRS 5158 – University of Burgundy – BP 47870 – 21078 Dijon cedex – France

⁴LEAD – UMR CNRS 5022 – University of Burgundy – Pôle AAFE – BP 26513 – 21065 Dijon cedex – France

⁵Department of Biosystems Engineering – Faculty of Bioscience Engineering- Ghent University – Coupure Links 653 - 9000 Gent – Belgium, Phone:+(32) 927 22 821, Bilal.Hijazi@ilvo.vlaanderen.be

CSBE101060 – Section III: Equipment Engineering for Plant Production Conference

ABSTRACT Centrifugal fertilizer spreaders are the most commonly used type in Europe. Their possible inaccuracy results in extra fertilizer being spread, which contributes strongly to environmental imbalance. This imbalance can only be corrected if the correct amount of fertilizer lands in the right place. Accuracy depends on understanding the spreading process from the vane to the soil. This knowledge enables the development of a feedback system that adjusts the spreader settings to the measured spread pattern. The spatial distribution of fertilizer granules on the soil can be predicted by a ballistic flight model based on the measurement of the velocities, directions, pellet size and angular distribution of the pellets. Several models have been proposed to meet this challenge. In an earlier study we proposed a standard camera and a strobe combined with a cross-correlation image- processing algorithm to determine the motion parameters of the pellets at ejection. This system is highly accurate for predicting spread patterns, but only for flat discs, as it only measures the 2D information of the ballistic flight of the pellets. Information on the third dimension will make this model more applicable in practice, as most centrifugal spreaders have concave discs. We developed a 3D image acquisition system based on stereoscopy to characterize the spreading process. Several tests were performed on simulated grain trajectories. Distances and vertical angles were measured with an error of less than 2%.

Keywords: fertilizer, centrifugal spreader, image processing, stereovision.

INTRODUCTION The environmental impact of fertilization and the associated nitrate pollution are since 1992 a matter of growing concern in Europe (EEC, 1992). Consequently, the control of the amount of fertilizer applied to a crop has become an important scientific issue. Several methods and models for the adjustment of centrifugal spreaders and for the control of the spreading pattern on the soil have been proposed.

Grift and Hofstee (1997) proposed an optical method to estimate the initial conditions of flight (velocity, direction) of the particles, their properties and geometrical parameters (topography, height and tilt of the discs, etc.). Subsequently, the spatial distribution of particles is calculated by introducing the initial conditions of flight in a ballistic model. However, this system provides only information for one individual granule and not for the entire flow and hence is not applicable under real fertilization conditions.

Cointault et al. (2002), Vangeyte and Sonck (2005) and Villette et al. (2007) proposed different techniques based on imaging systems. The first two techniques use for image acquisition a combination of a strobe lighting system and a low-speed camera. Cointault's system yields multi-exposure images with a large field of view (1x1 m²) which are treated by a MRF (Markov Random Field) based algorithm for motion estimation to determine the initial conditions of flight of the particles. However, the motion estimation algorithm based on MRFs did not provide a high accuracy (Hijazi et al., 2009).

On the other hand, Vangeyte's proposed imaging system has a 10x10 cm² field of view combined with a mechanical system to photograph the entire ejection area around the disc. An image processing algorithm is then applied on the images to obtain the trajectory of the particles. However, this system cannot be applied on a real-time fertilization in the field.

Villette et al. (2007) developed a method based on blurred images from which the outlet angles of particles can be determined. These angles are introduced in a simple mechanical model, taking into account only the behavior of one single granule, to calculate the spread pattern. The angular distribution of the fertilizer cannot yet be accurately determined. Furthermore, this method does not determine the granulometry of the fertilizer nor the behavior of the granules inside the vanes. This last parameter could allow to explain more accurately the behavior of the granules at the ejection.

Hijazi et al. (2009) improved Cointault's system with a new image processing algorithm based on cross-correlation to predict spread patterns, but only for flat discs, as it only measures the 2D information of the ballistic flight of the granules. Indeed, the motion of the particles is not parallel to the image plane and the millimeter-per-pixel conversion factor is not constant along the trajectory image on the CCD (Villette et al., 2008). Hence, information on the third dimension will make this model more applicable in practice, as most centrifugal spreaders are equipped with concave discs.

The long-term objective of our research is to use stereovision to determine the vertical displacement of fertilizer particles ejected by a centrifugal spreader. This paper describes a method and laboratory set-up to extract 3D information from grain trajectories. It also discusses the feasibility and precision of this method. We present the first results obtained with the new 3D imaging system based on stereovision applied on fertilizer particles.

MATERIALS AND METHODS Our application requires 3D information or depth perception and binocular stereopsis is a well-known and suited method for obtaining this information. This method recovers the three-dimensional objects location from two images recorded with different perspectives. This information cannot be determined from one single image (Barnard and Fischler, 1982). Stereovision theories use disparity or the difference in image location of an object seen by the left and the right camera to extract

depth information from two-dimensional images (Anderson and Nakayama, 1994). Firstly, we explain briefly the pinhole camera model and epipolar geometry as a theoretical background necessary to comprehend binocular stereovision. A more detailed description of stereovision concepts is found in (Faugeras, 2006).

The pinhole camera is modeled by an image plane, an optical center C and the focal length f which is the distance between C and the image plane. The projection point M of a world 3D point P into an image is the intersection of the line joining C and P (Figure 1).

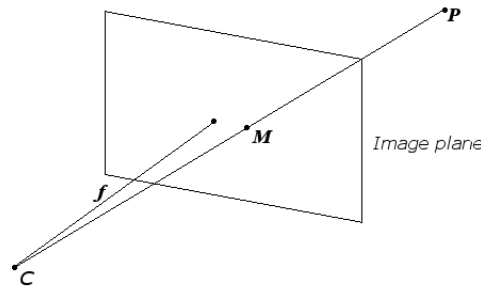


Figure 1: pinhole camera model

The projection of P in the image plane is represented in a linear transformation in the homogeneous coordinate which is called *perspective projection*. Let $p=[x \ y \ z]^T$ and $m=[u,v]^T$ be respectively the coordinates of P in the world reference and the coordinates of M in the image reference. Thus:

$$\begin{pmatrix} u \\ v \\ 1 \end{pmatrix} = PPM * \begin{pmatrix} x \\ y \\ z \\ 1 \end{pmatrix} \quad (1)$$

where PPM is the perspective projection matrix:

$$PPM = CM \begin{bmatrix} R | t \end{bmatrix} \quad (2)$$

The camera matrix CM depends on the intrinsic parameters only. R is the rotation matrix of the camera (orientation) and t is the translation vector, representing the rigid transformation from the camera reference frame to the world reference frame (Fusiello et al., 2000).

The epipolar geometry is explained in figure 2. Let us consider $M1$ and $M2$ as the projection of the point P in two images of a stereo rig composed of two pinhole cameras. Given a point $M1$ in the image plane 1, then its conjugate $M2$ in the image plane 2 has to lie on the epipolar line obtained by projecting the line containing $C1$ and $M1$ in the image plane 2. All the epipolar lines in an image pass through a common point called *epipole* which is the projection of the optical center of one camera in the image plane of the other camera. When the baseline, which is the line containing $C1$ and $C2$, is parallel with both

image planes, the epipoles are at infinity and the epipolar lines are parallel. A matching process is performed to look for the corresponding points in the left and right images. To reduce the search space to one dimension an alignment of the epipolar lines **or rectification** is necessary (Mallon and Whelan, 2005). Once the corresponding points $M1$ and $M2$ are known, the 3D position of the point P is the intersection between the lines $C1M1$ and $C2M2$.

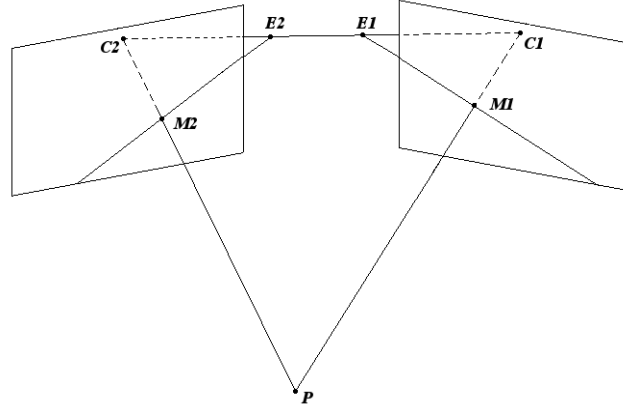


Figure 2: The epipolar geometry of a stereo rig. $C1$, $C2$, $E1$, $E2$, $M1$ and $M2$ are respectively the optical centers of the first and the second camera, the epipoles of the first and the second camera and the projection of point P on the first and the second image plane. $E1M1$ and $E2M2$ are respectively the epipolar lines of $M2$ and $M1$.

For our experiment a stereo rig composed of two high-resolution *Pike F-421B/C* cameras (2048 x 2048 pixels²) with two Pentax B1214D-2 lenses (12.5mm lens @F1.4-Close) is used. The orientation of the cameras is chosen in such a way that the intersection of their optical axes is equidistant from both cameras (750mm) (Figure 3.a). The calibration is done using the machine vision software (MVTec HALCON) and a 100x100 mm² calibration plate was used (Figure 3.b). After calibration three output files containing the intrinsic parameters of both cameras and the extrinsic parameters (mutual orientation of the cameras) are obtained. These parameters are used in both the undistortion and the rectification processes.

To model the lens distortion the division model is applied (Fitzgibbon, 2001). It models the radial distortions using one distortion coefficient (λ) (see eq. 3). Let P and x be respectively the perfect point and distorted version of P then the division model is written:

$$P = \frac{1}{1 + \lambda \|x\|^2} x \quad (3)$$

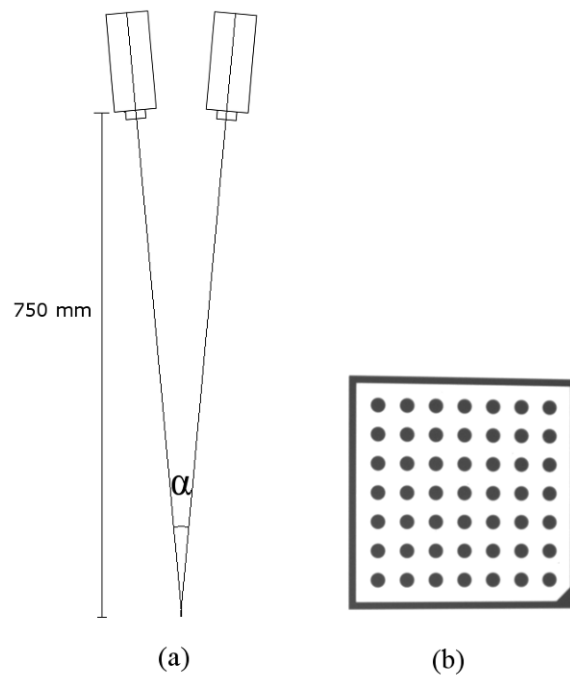


Figure 3: a) Stereo rig. b) 100x100mm² calibration plate.

To rectify the images a geometric model (Faugeras, 2006) is used. Theoretically, rectification consists of projecting the image stereo pairs on a common image plane parallel to the line $CIC2$ containing the optical centers of both cameras. Respecting this constraint ensures the alignment of epipolar lines in both images which is necessary to perform the matching between the images. However there exists an infinite number of planes parallel to $CIC2$. In the geometric model the new image plane is also parallel to the intersection of the old image planes and at equidistance from the old principal points, i.e. the projections of the optical centers.

Finally, for each pixel of an object in one image its conjugate in the other image needs to be determined to calculate the 3D position of this object in the world reference frame. In our experiment the matching was performed manually and the results were used to calculate the 3D coordinates.

To simulate the motion of one particle with a different known horizontal and vertical displacement (Figure 4) 3 particles were placed on a 20 cm long plate. The distances between particles and between the latter and the edges are 5 cm as shown in Figure 4. We performed tests with 3 vertical positions of the plate (2,37°; 4,76°; 7,15°).

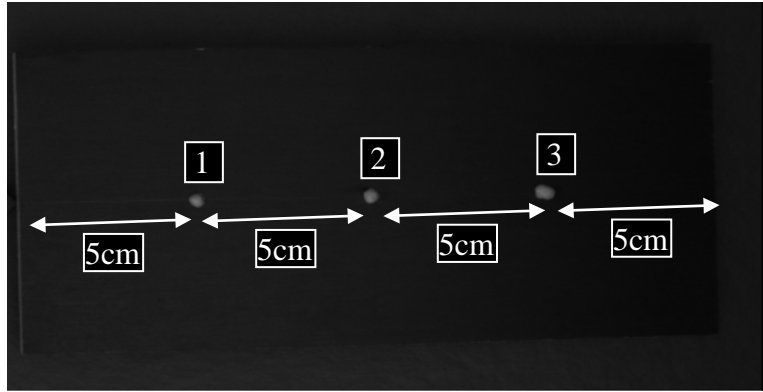


Figure 4: Knowing the exact dimension of the plate and the position of the particles on it enable to calculate the height of each particle.

In order to determine the influence of the 3D stereovision set-up on the measurement precision two configurations were tested, respectively with α equal to 10° and to 20° (Figure 3.a).

RESULTS AND DISCUSSION The results are presented in tables 1 and 2.

Table 1: Comparison between the calculated and real displacement and vertical angle with $\alpha = 10^\circ$

Case	Position	Displacement			Vertical angle		
		Calculated (m)	Real (m)	Error (%)	Calculated (degree)	Real (degree)	Error (%)
1	1-2	0,050767	0,05	1,534336	2,385963	2,378	0,31554
	2-3	0,050171	0,05	0,342882	2,398078	2,378	0,82492
2	1-2	0,051055	0,05	2,110294	4,654336	4,7610	2,24092
	2-3	0,049497	0,05	1,006019	4,819988	4,7610	1,23841
3	1-2	0,049429	0,05	1,142591	7,220944	7,1519	0,96565
	2-3	0,050692	0,05	1,384626	7,019374	7,1519	1,85278

Table 2: Comparison between the calculated and real displacement and vertical angle with $\alpha = 20^\circ$

Case	Position	Displacement			Vertical angle		
		Calculated (m)	Real (m)	Error (%)	Calculated (degree)	Real (degree)	Error (%)
1	1-2	0,050255	0,05	0,510464	2,376098	2,3784	0,099202
	2-3	0,05018	0,05	0,36081	2,379517	2,3784	0,044528
2	1-2	0,050303	0,05	0,605135	4,738589	4,7610	0,471279
	2-3	0,049999	0,05	0,001924	4,666518	4,7610	1,98506
3	1-2	0,050191	0,05	0,381091	7,201198	7,1519	0,689548
	2-3	0,049581	0,05	0,838891	7,136397	7,1519	0,216521

Tables 1 and 2 clearly demonstrate that the accuracy using the second configuration ($\alpha = 20^\circ$) is higher. Indeed, with $\alpha = 20^\circ$, the distance between the optical centers of both cameras is larger. That means for a point P in space that the disparity will be bigger with $\alpha = 20^\circ$ and the influence of the matching error is less, which leads to the better results obtained by the stereo rig with $\alpha = 20^\circ$.

In addition, the accuracy of the vertical angle depends on the displacement of the particles, the larger it is, the smaller the error is (eq.4).

$$vertical_angle = \arcsin\left(\frac{z_1 - z_2}{d}\right) \quad (4)$$

Where z_1 and z_2 are respectively the Z coordinate of a particle at the instant t and $t+\Delta t$ in the real world reference of which its (x,y) plane is the work plane.

Thus, to calculate the vertical outlet angle of a centrifugal spreader it is more accurate to calculate the angle between the disc and the farthest particles from it.

Furthermore, the accuracy of the method will be enhanced by replacing manual matching with an algorithm with sub-pixel precision.

CONCLUSION Since a high-speed vision system based on one camera is not sufficient to obtain information on the vertical displacement of fertilizer grains ejected by a concave spinning disc, the aim of this study was to assess the feasibility and the precision of a stereovision method. The basic principles of stereovision were briefly explained and then applied in our set-up with a simulated horizontal and vertical displacement of 3 particles. A precise calibration was performed, followed by an undistortion method and a rectification process. Finally, after a matching process between both images, the three-dimensional positions of the particles were calculated. The precision of the measured displacements and the angles were satisfying to use this method for further experiments. Moreover, the precision will be enhanced by applying a matching algorithm with sub-pixel precision

Since these results are promising for future work and after replacing the current cameras with high-speed cameras, this system will be compared with Grift's system.

Acknowledgements. The authors are indebted to Mr. Jan Van Mullem for his technical input.

REFERENCES

- Anderson, B.L. and K. Nakayama. 1994. Toward a general theory of stereopsis: binocular matching, occluding contours, and fusion. *Psychological Review*. (101): 414-445.
- Barnard, S.T. and M.A. Fischler. 1982. Computational stereo. *ACM Computing Surveys (CSUR)*. (14): 553-572.
- Cointault, F., M. Painsavoine, and P. Sarrazin. 2002. Fast imaging system for particle projection analysis: application to fertilizer centrifugal spreading. *Measurement Science and Technology* (13): 1087-1093.

- EEC. 1992. Council Regulation No. 2078/92 of 30 June 1992 on agricultural production methods compatible with the requirements of the protection of the environment and the maintenance of the countryside. Official Journal of the European Union L 215: 85.
- Faugeras, O. 2006. Three-Dimensional Computer Vision A Geometric Viewpoint. MIT press.
- Fitzgibbon, A.W. 2001. Simultaneous linear estimation of multiple view geometry and lens distortion.
- Fusiello, A., E. Trucco, and A. Verri. 2000. A compact algorithm for rectification of stereo pairs. *Machine Vision and Applications*. (12): 16-22.
- Grift, T.E. and J.W. Hofstee. 1997. Measurement of velocity and diameter of individual fertilizer particles by an optical method. *Journal of Agricultural Engineering Research*. (66): 235-238.
- Hijazi, B., F. Cointault, J. Dubois, S. Villette, J. Vangeyte, F. Yang, and M. Paindavoine. 2009. New high speed image acquisition system and image processing techniques for fertilizer granule trajectory determination. Joint International Agricultural Conference, Wageningen, Netherlands, 06-09 July.
- Mallon, J. and P.F. Whelan. 2005. Projective rectification from the fundamental matrix. *Image and Vision Computing*. (23): 643-650.
- MVTec HALCON. <http://www.mvtec.com/halcon>.
- Vangeyte, J. and B. Sonck. 2005. Image analysis of particle trajectories. the 1st International Symposium on Centrifugal Fertiliser Spreading, Leuven, Belgium.
- Villette, S., F. Cointault, P. Zwaenepoel, B. Chopinet, and M. Paindavoine. 2007. Velocity measurement using motion blurred images to improve the quality of fertiliser spreading in agriculture - art. no. 63560I, p. I3560-I3560. In: D. Fofi and F. Meriaudeau (eds.). Eight International Conference on Quality Control by Artificial Vision. Bellingham Spie-Int Soc Optical Engineering.
- Villette, S., E. Piron, F. Cointault, and B. Chopinet. 2008. Centrifugal spreading of fertiliser: Deducing three-dimensional velocities from horizontal outlet angles using computer vision. *Biosystems Engineering*. (99): 496-507.